

Structure and Barrier to Internal Rotation of Biphenyl Derivatives in the Gaseous State. Part 6. On the Molecular Structure and Internal Rotation of 2,2'-Bipyridine

Arne Almenningen,^a Otto Bastiansen,^{a,*} Snefrid Gundersen^a and Svein Samdal^b

^aDepartment of Chemistry, University of Oslo, P.O. Box 1033, Blindern, N-0315 Oslo 3 and ^bOslo College of Engineering, Cort Adelers gt. 30, N-0254 Oslo 2, Norway

Almenningen, A., Bastiansen, O., Gundersen, S. and Samdal, S., 1989. Structure and Barrier to Internal Rotation of Biphenyl Derivatives in the Gaseous State. Part 6. On the Molecular Structure and Internal Rotation of 2,2'-Bipyridine. – Acta Chem. Scand. 43: 932–937.

The gas-phase electron diffraction structure of 2,2'-bipyridine has been determined. Both static and dynamic models have been applied. The dynamic model is used to study the large-amplitude motion about the inter-ring C–C bond. The structure parameters ($r_a/\text{Å}$ and $\angle_a/^\circ$) for the dynamic model were found to be: $r(\text{C–C})_{\text{ave}} = 1.389(2)$, $r(\text{C–N})_{\text{ave}} = 1.352(4)$, $r(\text{C2–C2}') = 1.496(3)$, $r(\text{C–H})_{\text{ave}} = 1.108(3)$, and $\angle\text{C2}'\text{C2N1} = 116.1(5)$, $\angle\text{C2N1C6} = 116.2(7)$, $\angle\text{N1C6C5} = 124.6(6)$, $\angle\text{C2}'\text{C2C3} = 120.9(3)$. The numbers in parentheses are one standard deviation as given by least-squares refinement using a diagonal weight matrix. The most abundant stable conformation is the *anti* form. However, a less abundant conformation rotated about 120° from the *anti* form is indicated by both the static and dynamic models. The results obtained by the electron diffraction method are in good agreement with results both from X-ray and *ab initio* calculations. Experimental evidence suggests that the potential energy function for internal rotation about the inter-ring bond is different in the gaseous and liquid states, with a stronger stabilization of the *syn* form in the liquid state.

The chemistry and physical properties of bipyridines have been reviewed by Summers¹ up to mid-1982. Among the six different bipyridines, 2,2'-bipyridine has been most extensively studied. 2,2'-Bipyridine has found a wide range of applications in preparative and analytical chemistry owing to its ability to form metal complexes. The photophysics and photochemistry of these complexes are under active investigation, with particular interest in their application to solar energy conversion,² and as modelling intermediates in transition-metal catalyzed reactions.^{3,4} Bipyridines are also of interest in connection with their applications as the basis of herbicides,⁵ their use in obtaining new biologically active materials⁶ and their use in medicine.⁷ Finally, the importance of 2,2'-bipyridine as a building block in supramolecular chemistry⁸ should be mentioned.

The properties of 2,2'-bipyridine are closely related to its structure and conformation. 2,2'-Bipyridine is found to have a planar *anti* conformation in the solid state,⁹ while it takes a *syn* conformation in the complexes of transition metals. Mono- and dications of 2,2'-bipyridines are non-planar,¹ and this is supported by theoretical calculations.¹⁰ In solutions the dipole moment of 2,2'-bipyridine is non-zero,¹ and this has been interpreted by assuming a non-planar¹ structure. The interpretation of the NMR spectra is in accordance with an *anti*-like conformation.¹ However, a mixture of *anti* and *syn* conformations with a free energy

difference larger than 7.1 but less than 40.1 kJ mol⁻¹ has been proposed.¹¹ An early electron diffraction study finds the *anti* conformation as the most stable form, a shallow minimum at a non-planar *gauche* form and a maximum for the potential energy function at the planar *syn* form.¹² *Ab initio* calculations^{13–15} and semiempirical calculations^{1,16} predict the *anti* conformation to be the most stable form and a second *gauche*-like conformation as a less stable form.

We have previously successfully determined the molecular geometry and potential energy function for internal rotation for several biphenyl derivatives.^{17–21} A natural extension of this work is to incorporate *ortho*-substituted biphenyls and also biheterocyclic compounds such as bipyridines. The main purpose of this study is to gain further information about the molecular structure and potential energy function in the gaseous state for this important molecule.

Experimental

2,2'-Bipyridine was obtained from Aldrich and used without further purification.

The electron diffraction experiments were carried out with the Oslo apparatus²² for nozzle-to-plate distances of 476.61 and 196.66 mm, using Kodak Electron Image plates and a nozzle temperature of 125 °C. The wavelength of the electron beam was 0.06373 Å (estimated standard devia-

* To whom correspondence should be addressed.

tion of 0.1%), as calibrated against diffraction patterns of benzene using $r_a(\text{C}-\text{C}) = 1.3975 \text{ \AA}^{23}$ as standard. Six and five plates, respectively, were used for the long and short camera distances. The optimal densities (D) were recorded on a Joyce Loebel densitometer, and the densities were processed²⁴ using a blackness correction of $1 + 0.03D + 0.09D^2 + 0.03D^3$. A modification function $s/|f'_c|^2$ was applied, and a background subtraction program was used to subtract the background on the modified form. The program works essentially in the same way as that described by Hedberg.²⁵ The modified molecular intensity curves were averaged for each of the two camera distances, and these two average curves were used simultaneously in the least-squares analysis. The intensity data used in the structural analysis cover the range of $1.50 \leq s \leq 19.50 \text{ \AA}^{-1}$ with data intervals $\Delta s = 0.125 \text{ \AA}^{-1}$ for the 48 cm camera distance, and $7.50 \leq s \leq 44.00 \text{ \AA}^{-1}$ with $\Delta s = 0.25 \text{ \AA}^{-1}$ for the 20 cm camera distance.

The scattering amplitudes and phases were calculated using the partial wave method²⁶ based upon analytical Hartree-Fock potentials for C and N atoms, and the best electron density of bonded hydrogen for the H atoms.²⁷ The inelastic scattering factors were those of Tavard *et al.*²⁸

Structural analysis

The numbering of the atoms for 2,2'-bipyridine is shown in Fig. 2. The following independent structural parameters were selected to describe the molecular geometry: $r(\text{N1}-\text{C2})$, $r(\text{N1}-\text{C6})$, $r(\text{C2}-\text{C3})$, $r(\text{C3}-\text{C4})$, $r(\text{C4}-\text{C5})$, $r(\text{C5}-\text{C6})$, $r(\text{C2}-\text{C2}')$, $r(\text{C}-\text{H})_{\text{ave}}$, $\angle \text{C2}'\text{C2N1}$, $\angle \text{C2}'\text{C2C3}$, $\angle \text{C2N1C6}$, $\angle \text{N1C6C5}$ and Θ . The dihedral angle Θ about the central $\text{C2}-\text{C2}'$ bond is defined as 0° for the *anti* conformation. We have supposed the *anti* conformation to have C_{2h} symmetry, *syn* to have C_{2v} symmetry and all non-planar forms to have C_2 symmetry. Further, we have assumed that all the C-H bond distances are equal, and that each C-H bond bisects the adjacent CCC bond angle.

The structural analysis was carried out for both static and dynamic models. For the static model the torsional motion about the $\text{C2}-\text{C2}'$ bond distance was treated conventionally as a small-amplitude motion. The physical interpretation of the dihedral angle, Θ , determined by this model is an average angle which does not necessarily correspond to the minimum of the potential energy function about $\text{C2}-\text{C2}'$. The dynamic model treats the torsional motion as a large-amplitude motion where the potential energy function is explicitly included in the analysis.^{29,30}

According to the *ab initio* calculation the *anti* conformation is the most stable form. We therefore chose to express the potential energy function as a Fourier series [eqn. (1)], which has extremum points at $\Theta = 0^\circ$ (*anti*) and $\Theta = 180^\circ$ (*syn*). The interval between 0 and 180° was divided into ten sub-intervals, and the population in each sub-interval was calculated from $V(\Theta)$.

The asymmetry parameters κ for the bond distances were estimated³¹ according to $\kappa = au^4/6$ assuming³² $a = 2.0 \text{ \AA}^{-1}$

Table 1. u -Values (\AA) for some interatomic distances in 2,2'-bipyridine.

	r_a	Calculated	Static	Dynamic
N1-C2	1.35	0.0459	0.051	0.051 (1)
N1-C6	1.35	0.0456	0.051	
C2-C3	1.39	0.0464	0.052	
C3-C4	1.39	0.0464	0.052	
C4-C5	1.39	0.0464	0.052	
C2-C2'	1.50	0.0486	0.054	0.054 (3)
C-H	1.11	0.0770	0.085	0.085 (3)
N1...C2'	2.42	0.0640	0.062	0.061 (2)
N1...C3	2.41	0.0631	0.061	
N1...C5	2.42	0.0552	0.055	
C2...C3'	2.51	0.0638	0.063	
C2...C4	2.40	0.0560	0.055	
C2...C6	2.29	0.0555	0.055	0.052 (2)
C3...C6	2.38	0.0571	0.057	0.054 (2)
C4...C6	2.38	0.0557	0.055	0.054 (2)
N1...C4	2.81	0.0614	0.054	0.056 (5)
C2...C5	2.73	0.0609	0.054	
C3...C6	2.70	0.0629	0.056	
C2...C4'	3.77	0.0651	0.071	
C2...C6'	3.64	0.0655	0.071	
C2...C5'	4.22	0.0669	0.072	0.070 (8)
N1...C5'	4.98	0.0895	0.091	0.093 (6)
C5...C3'	5.06	0.0904	0.092	
C5...C4'	6.41	0.0878	0.099	0.095 (9)
C6...C5'	6.29	0.0876	0.098	
C5...C5'	6.95	0.0811	0.081	0.080 (2)

and using calculated u -values. The κ -values for all non-bonded distances were ignored.

Shrinkage is incorporated in the analyses by refining a consistent r_a -structure.³³

Calculation of u- and K-values. The force field given by Neto *et al.*,³⁴ excluding the interactions between out-of-plane and torsion, was used to calculate the root-mean-square amplitudes of vibration,³⁵ u -values, and the perpendicular correction coefficients, K -values. A program written by Hildebrandt *et al.*³⁶ was used for these calculations. For the static model the contribution from the torsional vibration is included, while the contribution from the torsional vibration is subtracted for the dynamic model to give framework u - and K -values, which were calculated for each of the ten sub-intervals. The calculated and observed u -values for the refined interatomic distances are given in Table 1.

$$V(\Theta) = 0.5V_1(1 - \cos \Theta) + 0.5V_2(1 - \cos 2\Theta) + 0.5V_3(1 - \cos 3\Theta) \quad (1)$$

Results and discussion

The final results for the static and dynamic models are given in Table 2 together with the optimised geometry from *ab initio*¹⁴ calculations, and structural parameters in the

Table 2. Structural parameters^a for 2,2'-bipyridine.

	Static	Dynamic	<i>Ab initio</i> ¹⁴	X-Ray ⁹
$r(\text{N1}-\text{C2})$	1.352	1.352 (4)	1.359	1.35
$r(\text{N1}-\text{C6})$	1.352 (5)		1.350	1.37
$r(\text{C2}-\text{C3})$	1.389	1.389 (2)	1.396	1.41
$r(\text{C3}-\text{C4})$	1.389		1.383	1.40
$r(\text{C4}-\text{C5})$	1.389	1.389 (2)	1.386	1.37
$r(\text{C5}-\text{C6})$	1.389		1.388	1.37
$r(\text{C2}-\text{C2}')$	1.498 (3)	1.496 (3)	1.512	1.50
$r(\text{C}-\text{H})$	1.105 (3)	1.108 (3)	1.082–1.087	
$\angle \text{C2}'\text{C2N1}$	116.1 (5)	116.1 (5)	116.4	116.1
$\angle \text{C2N1C6}$	116.6 (7)	116.2 (7)	116.2	116.7
$\angle \text{N1C6C5}$	124.3 (6)	124.6 (6)	124.3	124.3
$\angle \text{C2}'\text{C2C3}$	121.1 (3)	120.9 (3)	120.7	121.4
Θ_1	18.0 (2.7)	0.0	0.0	0.0
Θ_2	124 (16)	121	≈140	
% <i>anti</i>	93.1 (5.2)			
% <i>gauche</i>	6.9 (5.2)			
V_1		9.2 (11)		
V_2		5.7 (10)		
V_3		14.2 (10)		
R^b	4.33	4.35		

^aDistances are r_a (Å) and angles are \angle_a (°). Potential energy coefficients V in kJ mol^{-1} . Standard deviation (σ_{sq}) from the least-squares refinements when correlation among data and uncertainty in the electron wavelength are not included.

^b $R = 100[\sum w_i \Delta_i^2 / \sum I_i^2(\text{obs})]^{1/2}$, where $\Delta_i = I(\text{obs}) - I(\text{calc})$ and w_i is a weight function.

solid state.⁹ The correlation matrix corresponding to the dynamic model is given in Table 3. The modified molecular intensity curves for the dynamic model are shown in Fig. 1, and the corresponding radial distribution curves are shown in Fig. 2. An accurate molecular structure of the *anti* conformation corresponding to the dynamic model in Table 2 is shown in Fig. 3. Attempts to refine the four intra-ring C–C bond distances and the two C–N bond distances

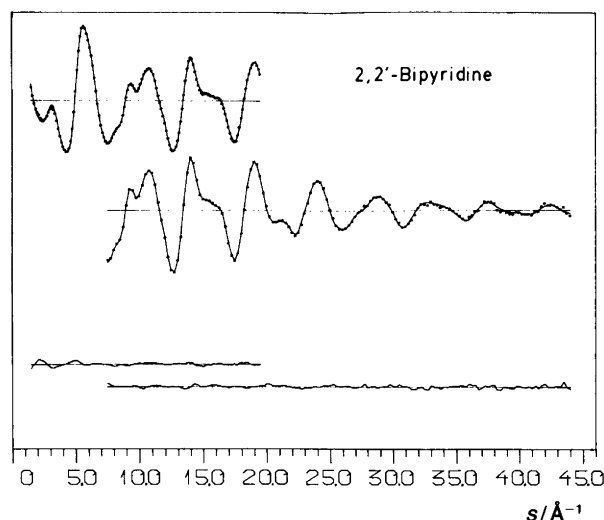


Fig. 1. Experimental (dots) and theoretical (full line) intensity curves, and the difference curves for 2,2'-bipyridine.

simultaneously and independently were not successful. Therefore the four C–C intra-bond distances were assumed equal, and the two C–N intra-bond distances were also assumed equal. Comparison with the *ab initio* results in Table 2 shows these assumptions to be reasonable.

Bond distances and angles. The geometrical parameters given in Table 2 for the static and dynamic models are almost identical, and the very small differences are well within the experimental uncertainties. They are also in excellent agreement with both the results of the *ab initio* calculations¹⁴ and X-ray results.⁹ The average intra-ring C–C bond distance, $r_a = 1.389$ Å, is found to be about 0.01 Å shorter than in benzene,²³ $r_a = 1.3975$ Å, and in pyridine,³⁷ $r_a = 1.397$ Å, while the average C–N bond distance, $r_a = 1.352$ Å, is about 0.01 Å longer than in pyridine,³⁷ $r_a = 1.342$ Å. The inter-ring C–C bond distance,

Table 3. Correlation matrix ($\times 100$) for the dynamic model for 2,2'-bipyridine. Only elements larger than 30 are included.

	1	2	3	4	5	6	7	8	9	10	11	12	13	14
1 V_1	100													
2 V_2	-96	100												
3 V_3	-34	100												
4 $r(\text{C}-\text{C})_{\text{ave}}$				100										
5 $r(\text{C2}-\text{C2}')$					100									
6 $r(\text{C}-\text{H})$						100								
7 $\angle \text{C2}'\text{C2N1}$			36	78	-44		100							
8 $\angle \text{C2N1C6}$				96			86	100						
9 $\angle \text{N1C6C5}$				-86			-75	-93	100					
10 $\angle \text{C2}'\text{C3C3}$				-72			-74	-73	71	100				
11 $r(\text{C}-\text{N})$				-98			-81	-95	84	74	100			
12 u_1^a				-95			-78	-92	82	71	95	100		
13 u_3				85			80	91	-91	-72	-84	-79	100	
14 u_4				48				49	-42	-57	-48	-46	43	100

^a u_1 , u_3 and u_4 represent groups 1, 3 and 4 in Table 1.

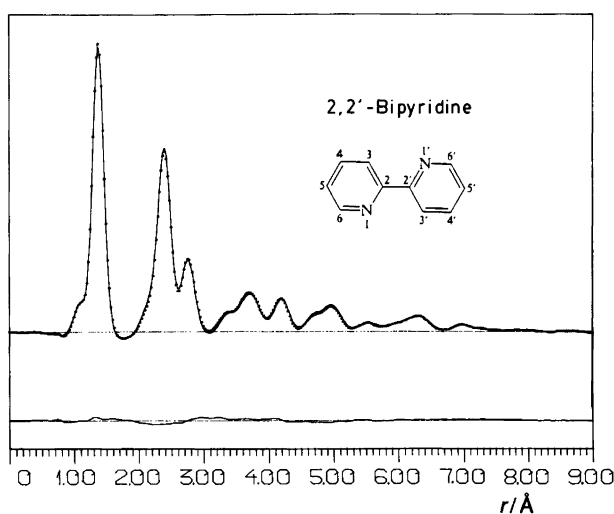


Fig. 2. Numbering of the atoms and experimental (dots) and theoretical (full line) radial distribution curves, and the difference curve for 2,2'-bipyridine. The artificial damping constant is $B = 0.0020 \text{ \AA}^2$. Theoretical intensities have been used below $s = 1.50 \text{ \AA}^{-1}$. Locations of some of the most important torsional independent distances are given in Table 1.

$r_a = 1.496 \text{ \AA}$, is similar to the inter-ring bond distances found in nine biphenyl derivatives,¹⁷⁻¹⁹ which vary from 1.480 to 1.513 \AA with an average value of 1.498 \AA .

All the bond angles determined by the electron diffraction method are in very good agreement with the results of the *ab initio* calculations¹⁴ and with X-ray results,⁹ as shown in Table 2. The $\angle\text{CNC}$ and $\angle\text{NCC}$ in pyridine³⁷ are 116.1 and 124.6°, respectively. Comparison of the values found for 2,2'-bipyridine, 116.2 and 124.6°, indicates no major changes in these angles due to substitution of another pyridine ring. There is a significant difference between the two angles $\angle\text{C2'C2N} = 116.1$ and $\angle\text{C2'C2C3} = 120.9^\circ$, which gives a tilt of the two pyridine rings in relation to the inter-ring C–C bond.

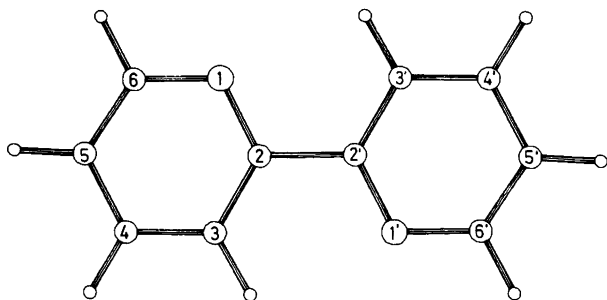


Fig. 3. An accurate molecular structure of the *anti* conformation corresponding to the parameters for the dynamic model given in Table 2.

Potential energy function. The static model gives two conformations with average torsional angles, $\Theta_1 = 18.0(2.7)$ and $\Theta_2 = 124(16)^\circ$, and relative abundances of 93(5) and 7(5)%, respectively, for the *anti* and *gauche* conformations. A value for $\Theta_1 > 0^\circ$ does not necessarily mean a non-planar *anti* geometry. The average torsional angle for the nitro group in *p*-bromonitrobenzene³⁸ is 18.8(2.3)°, where as nitrobenzene is found to be planar by microwave spectroscopy.^{39,40} The average torsional angle can be calculated from the potential energy function as:

$$\Theta_{\text{ave}} = \frac{\int_0^{180} \Theta P(\Theta) d\Theta}{\int_0^{180} P(\Theta) d\Theta}$$

where $P(\Theta) = \exp[-V(\Theta)/RT]$. Use of the Fourier coefficients given in Table 2 gives an average torsional angle of 18.8°, in excellent agreement with the value found from the static model. A second conformation corresponding to a *gauche*-like form is suggested from the experimental data by both the static and dynamic models and in agreement with *ab initio* calculations.^{13,15} However, the experimental uncertainties are too large for a definitive conclusion to be reached. These large uncertainties are of course closely related to the energy difference between the two conformations. A large energy difference gives low population and accordingly little information in the electron diffraction data. An increase in the nozzle temperature would increase the relative abundance of the less stable form.

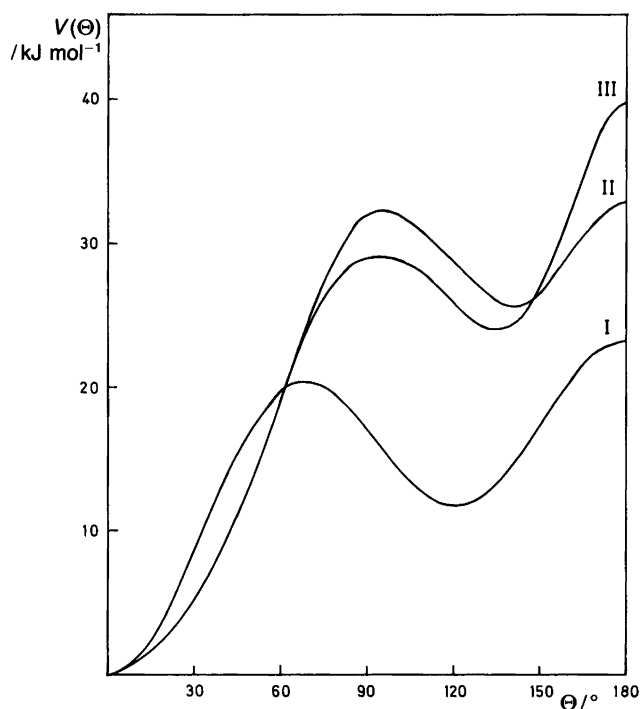


Fig. 4. Potential energy function about the inter-ring C–C bond for 2,2'-bipyridine. Curve I is derived from electron diffraction data, and curves II and III are *ab initio* results from Refs. 13 and 15, respectively.

Table 4. Some quantities^a related to the potential energy function of internal rotation about the inter-ring bond for 2,2'-bipyridine.

Method	Ref.	Θ_{\max}	$V(\Theta_{\max})$	Θ_{\min}	$V(\Theta_{\min})$	$V(\text{syn})$
ED	This work	67.7	21.5	121.1	11.3	23.4
<i>Ab initio</i> ^b	13	95	27.9	140	21.7	29.1
<i>Ab initio</i> ^b	15	98.7	29.3	136.8	22.9	39.7
<i>Ab initio</i>	14					26.7
NDDO ^{b,c}	16	100	23.9	138	20.9	26.7
Exp.	41				4.9–8.5	
Exp.	11				7.1–40.1	

^aThe quantities refer to the potential energy function shown in Fig. 3. Units are ° and kJ mol⁻¹. ^bPersonal correspondence.

^cInterpolated values using cubic spline functions with parabolic endpoints on nine values calculated by the NDDO method.

The potential energy function from the dynamic model is shown in Fig. 4 together with the functions calculated by *ab initio* methods.^{13,15} Quantities related to the potential energy function are summarized in Table 4. The overall agreement is good, but the theoretical calculations estimate the torsional angle for the second conformation to be about 15–20° larger than the electron diffraction results. Further, the potential energy curve from electron diffraction is much steeper around the *anti* conformation compared to the theoretical calculations. From the curvature of the potential energy function a torsional force constant can be calculated. Agresti *et al.*¹³ calculated the torsional frequency to be 37.5 cm⁻¹, which should be compared to the experimental³⁴ frequency of 73 cm⁻¹. In the vicinity of the *anti* conformation the relative population of molecules with small torsional angles is high. Therefore there is information about the curvature in the electron diffraction data, and indeed a steeper potential energy function as shown in Fig. 4 would give a higher torsional frequency, in better agreement with the experimental value. The torsional force constant, $k_{\Theta} = [dV(\Theta)/d\Theta]_{\Theta=0}$, calculated from electron diffraction data, is 0.133 mdyn Å rad⁻², which gives a calculated frequency of 81.0 cm⁻¹, whereas calculated from the *ab initio* calculation of Barone *et al.*¹⁵ it is 0.040 mdyn Å rad⁻², giving a torsional frequency of 56.9 cm⁻¹. The torsional force constant used by Neto *et al.*³⁴ is 0.105 mdyn Å rad⁻², which give a torsional frequency of 74.8 cm⁻¹. The observed torsional frequency³⁴ is 73 cm⁻¹.

Dipole moment. Because a non-zero dipole moment (0.6–0.9 D) has been found in solutions it has been suggested that the *anti* conformation is slightly non-planar.¹ Others⁴¹ have explained the non-zero dipole moment by assuming *anti* and *syn* conformations, and they have found the free energy difference between these two conformations to be between 4.9 and 8.5 kJ mol⁻¹ depending on the solvents used in the measurement of the dipole moment. A crude estimate of the dipole moment can be estimated from: $\mu = \mu_0 X_0 + \mu_{120} X_{120}$, where X_0 and X_{120} are the molar ratios, and μ_0 and μ_{120} the dipole moments at 0 and 120°, respectively. Using the composition found in the gaseous state and assuming $\mu_{120} \approx 2.7$ D gives a dipole moment of 0.2 D.

Another way of estimating the dipole moment would be to calculate the dipole moment from its variation with the torsional angle and the potential energy function [eqn. (2)].

$$\mu = \int_0^{180} \mu(\Theta) \exp[-V(\Theta)/RT] d\Theta / \int_0^{180} \exp[-V(\Theta)/RT] d\Theta \quad (2)$$

$\mu(\Theta)$ is not known, but its general form can be estimated by using a third-degree polynomial with the following constraints: $\mu(\text{anti}) = 0$ D, $\mu(\text{syn}) = 3.6$ D, $[d\mu/d\Theta]_{\text{anti}} = [d\mu/d\Theta]_{\text{syn}} = 0$. Using the potential energy function derived from electron diffraction and a temperature of 20°C gives a value for the dipole moment of only 0.003 D. The above considerations therefore suggest that the large non-zero dipole moment found in solution cannot be explained by a mixture of an *anti* and non-planar *gauche* conformations in solution alone. However, the relative abundance of the two conformations in solutions can be strongly influenced by interaction with the solvent, as Pawelka and Sobczyk⁴¹ have shown. Benedix *et al.*⁴² have found from NDDO calculations that a strong stabilization of the *syn* form can be expected in solution. Therefore the potential energy function can be quite different in the gas phase and in solution. If $V(\Theta)$ is multiplied by a factor of 0.2, i.e. stabilization of the *syn* form is assumed, the calculated dipole moment from the expression above would be 0.44 D.

Acknowledgement. The authors wish to express their gratitude to the Norwegian Research Council for Science and the Humanities (NAVF) and to the Board of Higher Education for Oslo and Akershus (RHOA) for financial support.

References

- Summers, L. A. In: Katritzky, A. R., Ed., *Advances in Heterocyclic Chemistry*, Academic Press, New York 1984, Vol. 35.
- Serpone, M., Pontarini, G., Jamieson, M. A., Bollett, F. and Maestri, M. *Coord. Chem. Rev.* 50 (1983) 209.
- Burton, J. T., Puddephat, R. J., Jones, M. L. and Ibes, J. A. *Organometallics* 2 (1983) 1487.

4. Scott, J. A. and Puddephat, R. J. *Inorg. Chim. Acta* 89 (1984) L26.
5. Eckhard, L. F., Keats, N. G. and Summers, L. A. *Z. Naturforsch. B* 33 (1978) 80.
6. Grant, H. G. and Summers, L. A. *Z. Naturforsch. B* 33 (1978) 118.
7. Kenny, A. D. and Morey, E. R. *J. Pharmacol. Exp. Theor.* 135 (1962) 317.
8. Lehn, J.-M. *Chem. Scr.* 28 (1988) 237.
9. Merritt, L. L., Jr. and Schroeder, E. D. *Acta Crystallogr.* 9 (1956) 801.
10. Hofmann, H.-J., Cimiraglia, R. and Tomasi, J. *J. Mol. Struct. (Theochem.)* 139 (1986) 213.
11. Murrell, J. N., Gil, V. M. S. and van Duijneveldt, F. B. *Recueil* 84 (1965) 1399.
12. Almennigen, A. and Bastiansen, O. *Kgl. Norske Vid. Selsk. Skr. No 4* (1958).
13. Agresti, A., Bacci, M., Castellucci, E. and Salvi, P. R. *Chem. Phys. Lett.* 89 (1982) 324 and personal correspondence.
14. Yagi, M., Makiguchi, K., Ohnuki, A., Suzuki, K., Higuchi, J. and Nagase, S. *Bull. Chem. Soc. Jpn.* 58 (1985) 252.
15. Barone, V., Minichino, C., Fliszár, S. and Russo, N. *Can. J. Chem.* 66 (1988) 1313 and personal correspondence.
16. Hofmann, H.-J. and Birner, P. *J. Prakt. Chem.* 327 (1985) 937 and personal correspondence.
17. Almennigen, A., Bastiansen, O., Fernholt, L., Cyvin, B. N., Cyvin, S. J. and Samdal, S. *J. Mol. Struct.* 128 (1985) 59.
18. Almennigen, A., Bastiansen, O., Fernholt, L., Gundersen, S., Kloster-Jensen, E., Cyvin, B. N., Cyvin, S. J., Samdal, S. and Skancke, A. *J. Mol. Struct.* 128 (1985) 77.
19. Almennigen, A., Bastiansen, O., Gundersen, S., Samdal, S. and Skancke, A. *J. Mol. Struct.* 128 (1985) 95.
20. Bastiansen, O. and Samdal, S. *J. Mol. Struct.* 128 (1985) 115.
21. Bastiansen, O., Gundersen, S. and Samdal, S. *Acta Chem. Scand. In press.*
22. Bastiansen, O., Hassel, O. and Risberg, E. *Acta Chem. Scand.* 9 (1955) 232.
23. Tamagawa, K., Iijima, T. and Kimura, M. *J. Mol. Struct.* 30 (1976) 243 and references therein.
24. Andersen, B., Seip, H. M., Strand, T. G. and Stølevik, R. *Acta Chem. Scand.* 23 (1969) 3224.
25. Hedberg, L. *5th Austin Symposium on Gas Phase Molecular Structure*, Austin, TX 1974, p. 37.
26. Yates, A. C. *Comput. Phys. Commun.* 2 (1971) 175.
27. Steward, R. F., Davidson, E. R. and Simpson, W. T. *J. Chem. Phys.* 42 (1965) 3175.
28. Tavad, C., Nicolas, D. and Rouault, M. *J. Chim. Phys.* 64 (1967) 540.
29. Seip, H. M. In: Sim, G. A. and Sutton, L. E., Eds., *Molecular Structure by Diffraction Methods*, Specialist Periodical Reports, The Chemical Society, London 1973, Vol. 1, Chap. 1, Part 1.
30. Fernholt, L., Rømming, C. and Samdal, S. *Acta Chem. Scand. A* 35 (1981) 707.
31. Kuchitsu, K. *Bull. Chem. Soc. Jpn.* 40 (1967) 498.
32. Kuchitsu, K. *Bull. Chem. Soc. Jpn.* 40 (1967) 505.
33. Kuchitsu, K. and Cyvin, S. J. In: Cyvin, S. J., Ed., *Molecular Structures and Vibrations*, Elsevier, Amsterdam 1972, Chap. 12.
34. Neto, N., Muniz-Miranda, M., Angeloni, L. and Castellucci, E. *Spectrochim. Acta, Part A* 39 (1983) 97.
35. Cyvin, S. J. *Molecular Vibrations and Mean Square Amplitudes*, Universitetsforlaget Oslo/Elsevier, Amsterdam 1968.
36. Hilderbrandt, R. L. and Wieser, J. D. *J. Chem. Phys.* 42 (1966) 4648.
37. Pyckhout, W., Horemans, N., Van Alsenoy, C., Geise, H. J. and Rankin, D. W. H. *J. Mol. Struct.* 156 (1987) 315.
38. Almennigen, A., Brunvoll, J., Popik, M. V., Vilkov, L. V. and Samdal, S. *J. Mol. Struct.* 118 (1984) 37.
39. Høg, J. H., Nygaard, L. and Sørensen, G. O. *J. Mol. Struct.* 7 (1970) 111.
40. Correll, T., Larsen, N. W. and Pedersen, T. *J. Mol. Struct.* 65 (1980) 43.
41. Pawelka, Z. and Sobczyk, L. *Bull. Acad. Pol. Sci.* 24 (1976) 961.
42. Benedix, R., Birner, P., Birnstock, F., Hennig, H. and Hofmann, H.-J. *J. Mol. Struct.* 51 (1979) 99.

Received March 13, 1989.